AIAA Paper 2008-25

Noise characteristics of overexpanded jets from convergent-divergent nozzles

K. B. M. Q. Zaman, [1]
NASA Glenn Research Center
Cleveland, OH 44135

Abstract

A broadband noise component occurring in the overexpanded flow regime with convergent-divergent nozzles is identified. Relative to a convergent nozzle, at same pressure ratios, this excess noise can lead to a large increase in the overall sound pressure levels. Several features distinguish it from the more familiar broadband shock associated noise. Unlike the latter, it is observed even at shallow polar locations and there is no noticeable shift of the spectral content in frequency with observation angle. The amplitudes are found to be more pronounced with nozzles having larger half-angle of the divergent section. The noise apparently occurs when a shock resides within the divergent section of the nozzle and results from random unsteady motion of the shock.

1. Introduction

Convergent-divergent nozzles run at off-design pressure-ratios often have noise components in addition to basic turbulent mixing noise. Two such components are well known: (1) screech tones and (2) broadband shock associated noise. Both originate due to interaction of turbulent flow structures with the quasi-stationary shock cells in the jet. The former involves a feedback loop – noise produced by vortical structures passing through a certain shock cell travels upstream and interacts with the nozzle lip to produce new vortical structures – rendering the flow periodic with accompanying emission of a sharp tone [1, 2]. Broadband shock associated noise (hereafter referred to as 'BBSN') also occurs due to interaction of the turbulent structures with the shock cells [2-5], except that there is no feedback loop involved. In this case, the aeroacoustic phenomenon may be represented by a distributed array of monopoles [3]. Time lag between the emitted noises from adjacent sources, in traveling to a stationary observer in the far field, explains such important characteristics as the variation of the frequency of the BBSN peak with the observer angle [2, 3]. Both screech and BBSN radiate most intensely in the forward arc (i.e., upstream direction). While screech usually does not occur in practical aircraft jets, BBSN can occur during cruise conditions becoming a source of annoying cabin noise [6, 7].

While noise components (1) and (2) may occur in both under- and overexpanded conditions (nozzle driving pressure higher and lower than design pressure, respectively), a third component, (3) also a sharp tone, may occur only in the overexpanded regime. This, referred to as 'transonic tone', was studied in detail in [8]. It is produced due to a resonance within the divergent section of the nozzle when a shock resides in that section. The part of the nozzle downstream from the shock behaves similarly as a one-quarter wave resonator (like a pipe section closed on one end and open on the other) often producing resonance at the fundamental or its odd harmonic frequencies. As pertinent, components (1)-(3) will be elaborated further in the following. The objective of this paper is to discuss the possible presence of a fourth component, (4), that is broadband in nature and occurs also only in the overexpanded regime.

[1] Aerospace Engineer, Inlet & Nozzle Branch, Aeropropulsion Division, AIAA Associate Fellow.

Since component (4) is broadband, in order to differentiate it from the other broadband component (BBSN), it is important to first review the characteristics of the latter. Figure 1 shows narrow band spectra at different observer angles taken from [9] (see also [2]). The angular location, θ, is measured with respect to the downstream jet axis. The data are from a C-D nozzle with design Mach number of 1.5. At each θ, there are three curves and the sets of curves are staggered vertically for uncluttered viewing. First, let us compare data for the underexpanded case (M_j = 1.67; blue, long-dash curve) with that for the design condition (M_j = 1.49; red, small-dash curve). For the former case there is a screech tone, seen clearly as a spike in the spectra at the largest θ location. In addition to the screech there is also a broad peak, marked by a downward-pointing arrow, at a higher frequency. This represents the broadband shock noise, BBSN. A salient feature of it is that the frequency of the peak increases as θ decreases. It is prominent at large θ locations and with decreasing θ the peak broadens and the amplitude diminishes. At shallow angles it would be hardly detectable and the spectra would be similar to that of the fully expanded case.

While data found in the literature on BBSN pertain mostly to underexpanded flows, limited data exist for overexpanded flows [9]. The comparison in Fig. 1 includes an overexpanded case (M_j = 1.28; light blue, solid curve). A scrutiny reveals that both screech and BBSN occurs for this condition. The BBSN peaks are marked by upward-pointing arrows. Importantly, the trends of the BBSN with varying θ can be seen to be practically the same as that already discussed for the underexpanded case. Analytical models, e.g., provided in Ref. [3, 2], predict the frequency of the BBSN peak and its variation with θ well.

Figure 2 illustrates the impact of BBSN on overall sound pressure level. Following the representation in [5], data trends for OASPL are shown schematically as a function of M_j for a location where BBSN is prominent (say, θ = 90°). The dotted line (purple) represents turbulent mixing noise. This curve would be obtained if at each M_j an appropriate C-D nozzle were used to obtain perfectly expanded flow. Result from a convergent nozzle is represented by the dashed (blue) curve while that from a given C-D nozzle (having same throat diameter as the convergent case) is shown by the solid (green) curve. At the design Mach number (fully expanded condition), the C-D nozzle has noise due only to turbulent mixing. On either left (overexpanded condition) or right (underexpanded condition) of this point, the C-D nozzle exhibits higher levels due to BBSN. The convergent nozzle does not exhibit a dip in the middle because the flow is underexpanded and accompanied by BBSN everywhere in the range $M_j > 1$. In similar schematics (as in Fig. 2) shown earlier by Tam [2, 5], the intensity levels for the convergent nozzle were shown to coincide with those for the C-D nozzle on the low end of the M_j-range. However, their focus was on higher M_j and they did not pay attention in the range of M_j below about 1.2. It is in this range of M_j we do an inspection in this investigation. It will be demonstrated that the C-D nozzle intensities are actually much larger than the convergent case, as sketched by the small-dash line (red). The higher intensities are due to the noise component (4) which, for lack of a better term will be referred to simply as ‘excess noise’ in the following. The main objective of this paper is to present data from several model-scale nozzles demonstrating clearly the presence of this excess broadband noise. It will be reasoned that like component (2) is similar in morphology to (1) but without a feedback loop, the mechanism of (4) might be similar to that of (3) without a feedback loop.

2. Experimental Procedures

All data are obtained in a small open jet facility at NASA Glenn Research Center (Fig. 3a). Compressed air enters through one end of a 12.7 cm diameter cylindrical plenum chamber and exhausts through a nozzle fitted on the other end. The jet discharges into the ambient of the test chamber. The data are for cold flow, i.e., the total temperature everywhere is approximately the same as the ambient temperature. The sound pressure data are obtained

by two microphones held fixed at angular locations of ($\theta \approx$) of 25° and 90°, relative to the downstream jet axis. Spectral analysis is done with a Nicolet 660B analyzer.

Data for several convergent-divergent nozzles are acquired. The nozzles in Fig. 3(b), used in the earlier study [8] and denoted as '6T2', '3T2' and '7T2', have the same throat diameter (D_t) and length (L) while the exit diameter (D_e) is varied. Nozzles 'M22', 'M28' and 'M36', in Fig. 3(c), have the same throat diameter and divergence angle while the length is varied. The divergent parts of the latter nozzles screw on to the same convergent part. The dimensions of the six nozzles (in mm, see Fig. 1d for notations) are listed in Table 1; here, M_D represents the design Mach number based on the throat-to-exit area ratio and φ represents the half-angle of divergence in degrees.

Table 1 Details of the nozzles used in the study; dimensions in mm.

Noz	D_t	D_e	L	M_D	φ
6T2	7.62	8.1	19.1	1.14	0.72
3T2	7.62	10.2	19.1	1.78	3.85
7T2	7.62	12.7	19.1	2.78	7.60
M22	6.35	9.22	10.1	2.26	8.00
M28	6.35	11.7	19.0	2.77	8.00
M36	6.35	17.2	38.5	3.58	8.00
CV1	14.5	14.5	6.35	1.00	0.00

Data with convergent nozzles are also taken as the 'baseline' case for the comparison. For the final convergent case chosen ('CV1'), a tab is used to suppress screech (see next section). The 'fully expanded jet Mach number', $M_j = (((p_0 / p_a)^{(\gamma-1)/\gamma} - 1)\frac{2}{\gamma - 1})^{1/2}$, is used as the independent variable; here, p_0 and p_a are plenum pressure and ambient pressure, respectively. Note that for supersonic flows M_j is simply a function of nozzle pressure ratio and represents a Mach number at the nozzle exit had the flow expanded fully.

3. Results

In order to provide the reader with a clear sense of the operating regimes as well as the nature of the transonic tones, Fig. 4 is reproduced from Ref. [8]. The frequencies of the sharp tones, observed with nozzle 3T2, are plotted while the driving pressure (and thus, M_j) is varied. The band of frequency data on the right represents screech while there are two stages of transonic tones on the left, as indicated. The vertical lines in this figure demarcate flow regimes determined from one-dimensional nozzle flow analysis, based simply on the throat-to-exit area ratio. From the left, the first line (dashed, I) represents the condition when the flow is just choked, the second line (dotted, II) when a 'normal shock' is just pushed out of the nozzle exit, and the third line (chain-dashed, III) when the flow is perfectly expanded. Thus, to the left of the dashed line (I) the flow is subsonic, between the dashed and dotted lines (I-II) a shock is expected in the divergent section, between the dotted and the chain-dashed lines (II-III) the flow is overexpanded, and to the right of the chain-dashed line (III) the flow is underexpanded. While boundaries I and III are well represented, it turns out that boundary II is grossly underpredicted by 1-D analysis. In reality, for nozzle 3T2 boundary II is actually located to the right at location II' (reader may look up [8] for further details).

Thus, the transonic tones occur in the regime bounded by I and II' when a shock resides within the divergent section of the nozzle. The broadband noise under consideration also appears to takes place within this same flow regime, as elaborated in the following. It should be mentioned here that the flow coming out of the nozzle in

the regime bounded by I and II', in the sense of one-dimensional analysis, may be expected to be subsonic and true overexpanded flow may be expected only in the range II'-III. In reality, however, when a shock resides within the nozzle the flow downstream usually separates and the ensuing jet has characteristics similar to that of an overexpanded jet [8,10]; hence the justification of the term 'overexpanded' in this paper.

In order to study the broadband noise it is desirable that tones are not present. The transonic tones have been shown to be characteristic of nozzles with polished interiors. Suitable boundary layer tripping often suppresses the tones. This is shown in Fig. 5 for nozzles 3T2 and 7T2. The trip was applied upstream of the throat making sure that the throat area did not change. The spectral data are for $M_j \approx 0.95$. It can be seen that with either nozzle, without boundary layer trip, there is a strong transonic resonance. This is almost completely suppressed by the trip. However, residual tones sometimes persist even with the trip, as apparent by the presence of a small peak on the left in Fig. 5(b). In the following, all data with the C-D nozzles are taken with the application of similar boundary layer trips.

For an assessment of the 'baseline' case, SPL spectra were acquired and examined for three different convergent nozzles. The three had exit diameters of 14.5, 12.7 and 6.5 mm. Spectra for these cases are shown in Fig. 6. The data are referenced to the largest diameter (14.5 mm). The r.m.s. pressure fluctuation p' scales as, $(p'/\rho_j U_j^{\,2})^2 (r/D)^2 (U_j/(\Delta f D))$; [11]. Thus, for same jet velocity, microphone distance and bandwidth (Δf), the amplitude is converted as,

$$SPL_1 = SPL_2 + 20\log_{10}\left(\frac{D_1}{D_2}\right) - 10\log_{10}\left(\frac{D_2}{D_1}\right). \qquad (1)$$

The frequency is nondimensionalized into Strouhal number, fD/U_j; U_j being the 'fully expanded' jet velocity corresponding to M_j. It can be seen that the data have collapsed reasonably well; the smaller nozzles exhibit somewhat lower levels presumably due to larger boundary layer thickness relative to the nozzle diameter. Data from the largest case (CV1) is used in the following as baseline. The C-D nozzle data are compared with the CV1 data after conversion with Eq. (1) based on the throat diameter.

There is another consideration with the convergent nozzle before proceeding with the main results of this paper. Screech occurring for $M_j > 1$ with the convergent nozzle also poses a problem in the comparisons. This can lead to wrong inferences especially when comparing overall sound pressure levels (OASPL). Fortunately a technique exists for suppressing screech that was also used in previous experiments [4, 9]. A tab placed on the periphery of the nozzle effectively suppresses the screech tones. This is shown in Fig. 7. It can be seen that while the tab does not significantly affect the spectra at subsonic conditions ($M_j = 0.95$; top graph), it eliminates screech at $M_j = 1.2$ and 1.42 (middle and bottom graphs). Thus, comparisons are made in the following with data taken from the C-D nozzles with boundary layer trip and the convergent nozzle with a tab, after data conversion in the format of Fig. 6 by Eq. (1). It will be seen that some residual transonic tones and screech remained but their effects were deemed negligible in the comparative study. On the other hand, screech took place with some C-D nozzles (prominently with the ones having small divergence angle). A tab was tried with nozzle 3T2 and found to be practically ineffective in suppressing screech. (A possible explanation may be found in [12]. For the flow regimes considered, there is an adverse streamwise pressure gradient within the divergent section. This counters the formation of a 'pressure hill' necessary for generation of streamwise vortices by the tab, leading to the ineffectiveness.) Thus, tabs were not used with any of the C-D nozzles and screech occurred with some of them; this should be borne in mind while interpreting the comparative results.

Figure 8 compares noise spectra for nozzle 6T2 and the convergent case, at $\theta = 90°$. Data are shown for five different values of M_j. Nozzle 6T2 has the least divergence and the differences in the broadband levels with the

convergent case are small in most of the cases. However, a prominent increase in the levels is clear at M_j = 0.95 where the flow is overexpanded. At the higher M_j's, 6T2 involves underexpanded flow and is marked by strong screech as can be seen in the lower three graphs of Fig. 8.

Data for nozzles 3T2 and 7T2 are shown similarly in Figs. 9 and 10, respectively. For nozzle 3T2 (Fig. 9), the increases in the broadband levels are more pronounced relative to the 6T2 case; compare data at the lower M_j's between Figs. 9 and 8. Note that there is residual transonic tone at the lowest M_j and screech appears at the highest M_j with 3T2. Throughout the M_j-range the flow is either overexpanded or a shock resides within the divergent section for this nozzle (see discussion of Fig. 4). Nozzle 7T2 also involves similar flows as the 3T2 case. The latter has the largest divergence angle and the increase in the broadband levels at the lower M_j conditions (Fig. 10) is found to be the most pronounced. Here, only minor residual transonic tone is noted and screech is absent at all M_j. Thus, the differences in the noise for the 7T2 case are in essence unambiguously due to increases in the broadband components and not influenced by tones.

BBSN can be identified in some of the spectra for the convergent nozzle at $\theta = 90°$. In Fig. 9 the corresponding peaks are marked by the upward-pointing arrows. The frequency of the peak occurs at Strouhal numbers of 1.15, 0.65, and 0.45 for M_j = 1.20, 1.42 and 1.59, respectively. For nozzle 3T2 while BBSN appears at M_j = 1.42, the spectra being curiously identical to that of the convergent case, it may be buried under the influence of screech at the highest M_j. At the lower values of M_j, BBSN is not detected with the C-D cases.

While the data in Figs. 8-10 are for $\theta = 90°$, corresponding data at shallow angle ($\theta = 25°$) are shown only for nozzle 3T2, as an example, in Fig. 11. Similar trends are noted. An increase in the broadband levels is observed at the lower M_j cases; compare with data in Fig. 9. The fact that increased levels are also observed at shallow angles distinguishes the excess noise under consideration from BBSN. Recall that BBSN decreases in amplitude with decreasing θ and can hardly be noted at shallow angles. Furthermore, by comparison of the data at the two angular locations, it can be seen that the excess spectral content does not appear to shift in frequency. In most cases, the increase in the levels occurs at lower frequencies with a shift of the entire spectra to higher levels. It is also noted in Fig. 11 that, with screech occurring at the highest two M_j cases, the broadband levels are actually lower with the C-D nozzle. Thus, for the three nozzles considered, the increase in the broadband levels occur at relatively lower M_j (<1.2) for both θ-locations. The overall trends are reflected in the OASPL data shown next.

Figure 12 shows overall sound pressure level, computed by integration of the spectra, as a function of M_j for the two angular locations. Up to about M_j = 1.2, relative to the convergent case, the levels are significantly larger with the C-D nozzles. It is apparent that the increase in the levels is more with increasing divergence of the nozzle. The spectral data discussed in the foregoing make it clear that the increases in the OASPL are due mainly to increases in the broadband levels; this is particularly true for nozzle 7T2 which involves broadband spectra without sharp peaks. The excess broadband noise leading to an increase in OASPL is distinct from BBSN as discussed earlier. The increases in the levels are large, for example, by as much as 14 dB in OASPL at M_j = 0.8 and $\theta = 90°$. Finally, Figure 13 documents OASPL data obtained with the nozzles having the same divergence angle but different lengths (Table 1). A similar trend of increased OASPL, due to an increase in the broadband levels, is also seen clearly with these nozzles.

4. Discussion and Summary

In this paper a broadband noise component occurring in the overexpanded flow regime of supersonic jets from convergent-divergent nozzles is identified. Relative to a convergent nozzle, this additional noise can lead to a large increase in overall sound pressure level, by as much as 14 dB noted in certain cases. Several features distinguish it from the more familiar broadband shock associated noise. Unlike BBSN, it is observed even at shallow

polar locations. Also, the excess levels occur at lower frequencies and there is no noticeable shift of the spectral content with observation angle. With the limited data at hand, the excess noise is found to be more pronounced with nozzles having larger half-angle of the divergent section. The excess noise takes place roughly in the same M_j -range where transonic tones would be expected with a smooth interior of the nozzle. This leads to the belief that the mechanism of the excess noise traces to unsteady shock motion within the divergent section. With a smooth interior, providing azimuthal symmetry, the unsteady shock motion locks on to a resonance generating the transonic tones. With a larger practical nozzle, or boundary layer trip with the model-scale nozzles, a breakdown in azimuthal symmetry apparently prevents the resonance leading to a random unsteady motion. The latter gives rise to the observed increase in the noise levels that are broadband in nature. It is possible that the excess noise under consideration and the BBSN component are mutually exclusive. With a given C-D nozzle when one occurs the other may not. The component BBSN occurs when the shock from inside the divergent section is pushed out and a periodic train of strong shocks is formed outside the nozzle. The excess noise component occurs at lower pressure ratios when the shock is inside.

How relevant is this excess noise in practical applications? Since it occurs at lower pressure ratios at the onset of the overexpanded regime, it may not be of concern in typical flight conditions. However, there could be situations, e.g., the climb-to-cruise stage of certain fighter jets when the engine involves overexpanded exhaust [13-15], where it might be relevant. It is needless to say, however, that one must be aware of its existence especially in efforts to simulate and predict supersonic jet noise accurately.

Acknowledgement

Support from the Supersonics Projects of the Fundamental Aeronautics Program is gratefully acknowledged. Thanks are due to Dr. James Bridges for providing helpful inputs during the course of the study, and also to Dr. Nicholas Georgiadis and Prof. Phillip Morris for providing constructive comments on the manuscript.

References

[1] A. Powell, "On the mechanism of choked jet noise," *Proc. Phys. Soc. London*, 66, pp. 1039-1056, 1953.

[2] C.K.W. Tam, "Supersonic jet noise," *Ann. Review Fluid Mech*., **27**, pp. 17-43, 1995.

[3] M. Harper-Bourne and M.J. Fisher, "The noise from shock waves in supersonic jets," *Proc. AGARD Conf. on noise mechanisms* (No. 131), Brussels, Belgium, 1973.

[4] H.K. Tanna, "An experimental study of jet noise part II: shock associated noise," *J. Sound and Vib.*, **50**(30), pp. 429-444, 1977.

[5] C.K.W. Tam and H.K. Tanna, "Shock associated noise of supersonic jets from convergent-divergent nozzles," *J. Sound & Vib*., **81**(3), pp. 337-358, 1982.

[6] K. Viswanathan, "Parametric study of noise from dual-stream nozzles," *J. Fluid Mech*., **521**, pp. 35-68, 2004.

[7] O.H. Rask, E.J. Gutmark and S. Martens, "Broadband shock associated noise suppression by chevrons," *AIAA Paper* 2006-9, 44th Aerospace Sciences Meeting, Reno, NV, 9-12 Jan., 2006.

[8] K.B.M.Q. Zaman, M.D. Dahl, T.J. Bencic and C.Y. Loh, "Investigation of a 'transonic resonance' with convergent-divergent nozzles," *J. Fluid Mech*., **462**, pp. 313-343, 2002.

[9] T.D. Norum and J.M. Seiner, "Measurements of mean static pressure and far-field acoustics of shock-containing supersonic jets," *NASA TM* 84521, September, 1982.

[10] C.A. Hunter, "Experimental, theoretical and computational investigation of separated nozzle flows", *AIAA Paper* 98-3107, 1998.

[11] K.B.M.Q. Zaman and J.C. Yu, "Power spectral density of subsonic jet noise," *J. Sound and Vib.*, **98**, pp. 519-537, 1985.

[12] K.B.M.Q. Zaman, M.F. Reeder, and M. Samimy, "Control of an axisymmetric jet using vortex generators," *Physics of Fluids A*, **6**(2), pp. 778-793, 1994.

[13] B. Greska, A. Krothapalli, and V. Arakeri, "A further investigation into the effects of microjets on high speed jet noise," *AIAA Paper* 2003-3128, 9th AIAA/CEAS Aeroacoustics Conference, Hilton Head, SC, 12-14 May, 2003.

[14] T.D. Norum, D.P. Garber, R.A. Golub, O.L. Santa Maria and J.S. Orme, "Supersonic jet exhaust noise at high subsonic flight speed," *NASA TP* 2004-212686, January, 2004.

[15] J.M. Seiner, B.J. Jansen and L.S. Ukeiley, "Acoustic fly-over studies of F/A E/F Aircraft during FCLP mission", *AIAA Paper* 2003-3330, 9th AIAA/CEAS Aeroacoustics Conference, Hilton Head, SC, 12-14 May, 2003.

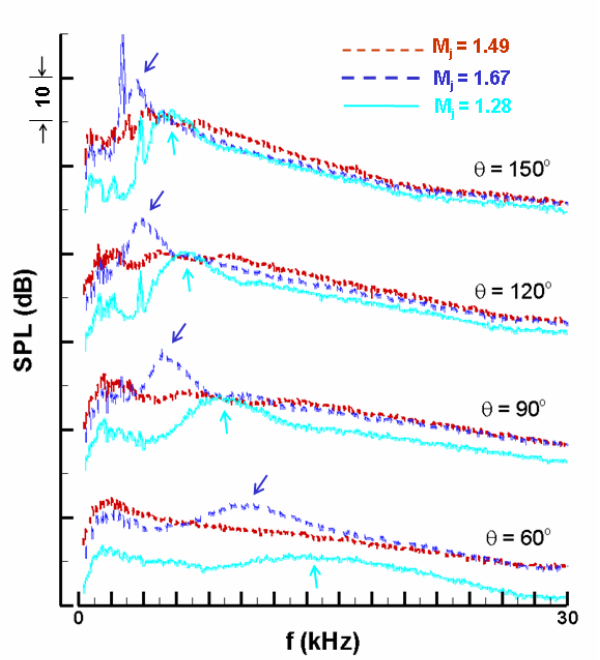

Fig. 1 Sound pressure level spectra for a M_D = 1.5 C-D nozzle at different polar locations (θ), from Ref. [9]. At each θ the three curves are for 'fully expanded Mach numbers' of 1.67, 1.49 and 1.28. Sets of curves are staggered vertically.

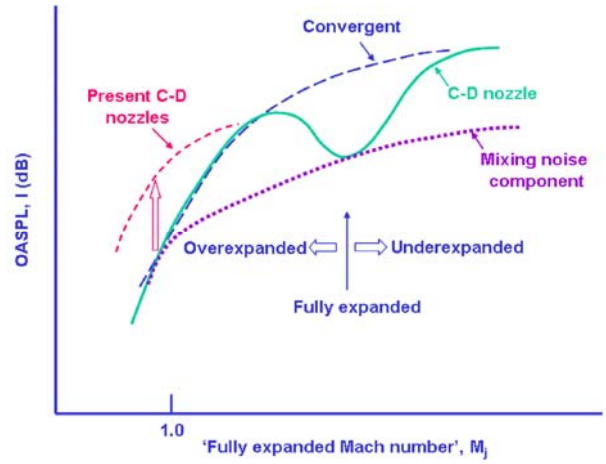

Fig. 2 Schematic of OASPL vs. M_j for C-D nozzle versus Convergent nozzle, after Ref. [5].

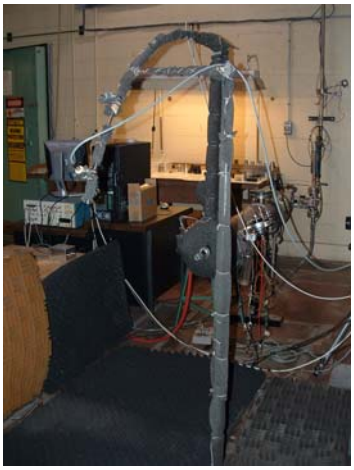

(a)

(b)

(c)

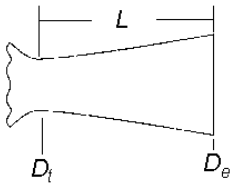

(d)

Fig. 3 Experimental setup: (a) open jet facility, (b) nozzles 3T2, 6T2 and 7T2, (c) nozzles with 16° conical divergent section, (d) schematic of interior of all nozzles.

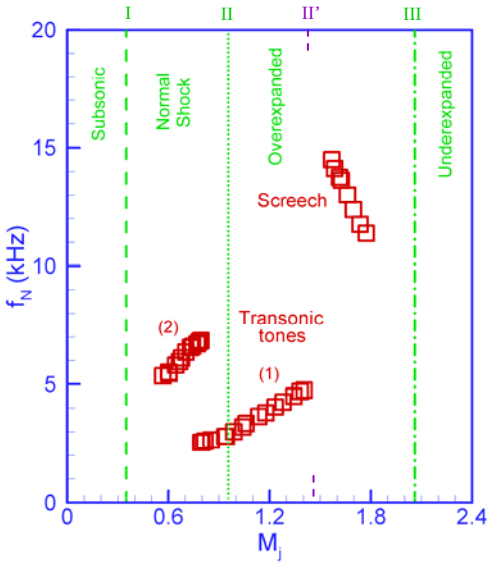

Figure 4 Variation of frequencies of transonic tone and screech with M_j for nozzle 3T2 from Ref. [8].

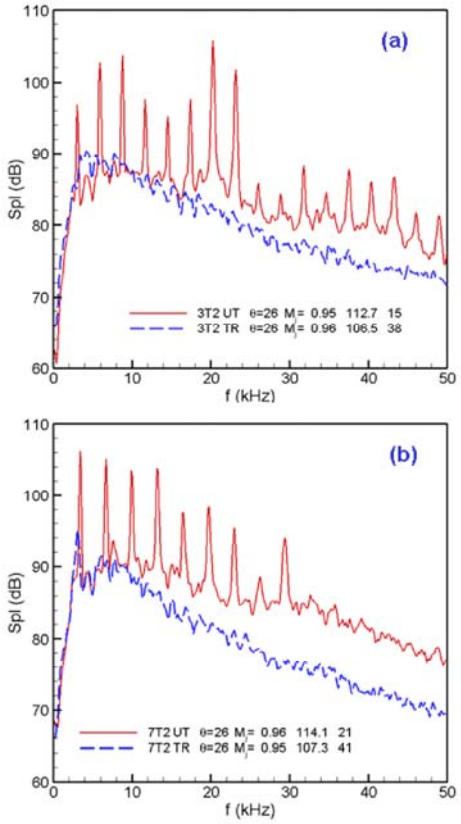

Fig 5 Comparison of SPL spectra with and without boundary layer trip at $\theta = 25°$: (a) Nozzle 3T2, (b) nozzle 7T2.

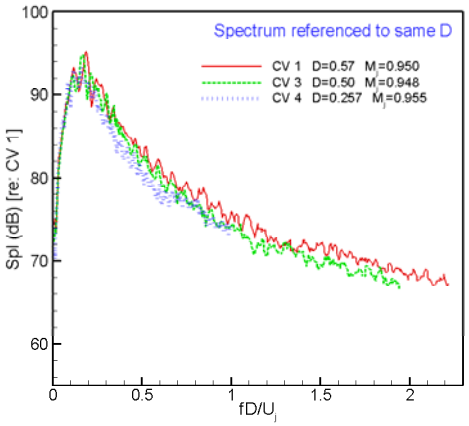

Fig. 6 SPL spectra for three convergent nozzles with diameters of 14.5, 12.7 and 6.5 mm; spectra referenced to D=14.5 mm.

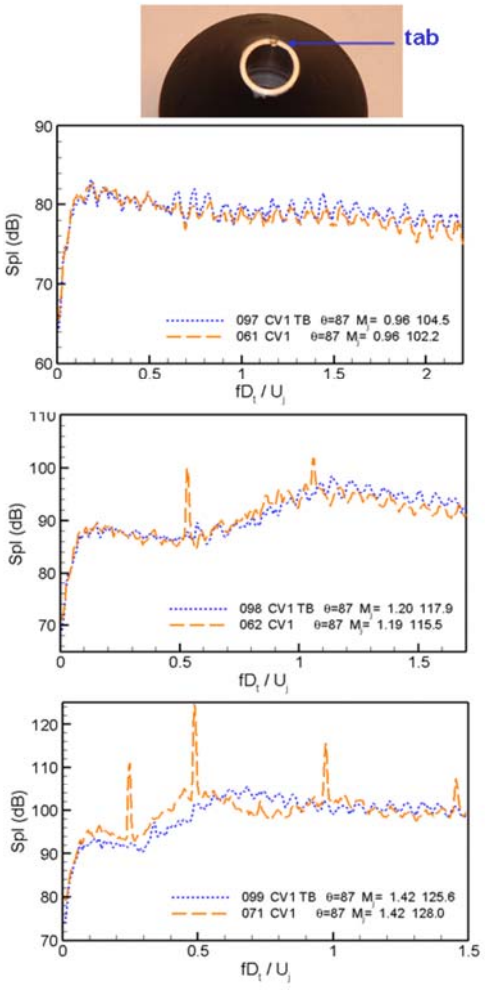

Fig. 7 SPL spectra for convergent nozzle (CV1) with and without a tab, $\theta = 90°$.

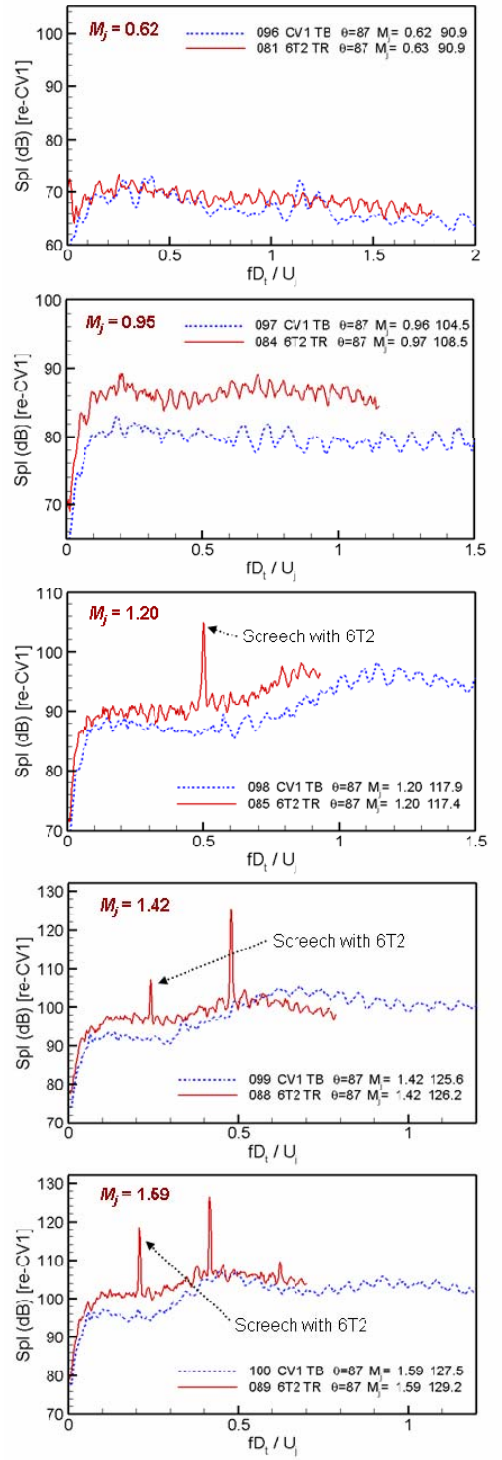

Fig. 8 SPL spectra for nozzle 6T2 (M_D = 1.14) vs. convergent (CV1) case, at indicated M_j; θ = 90°.

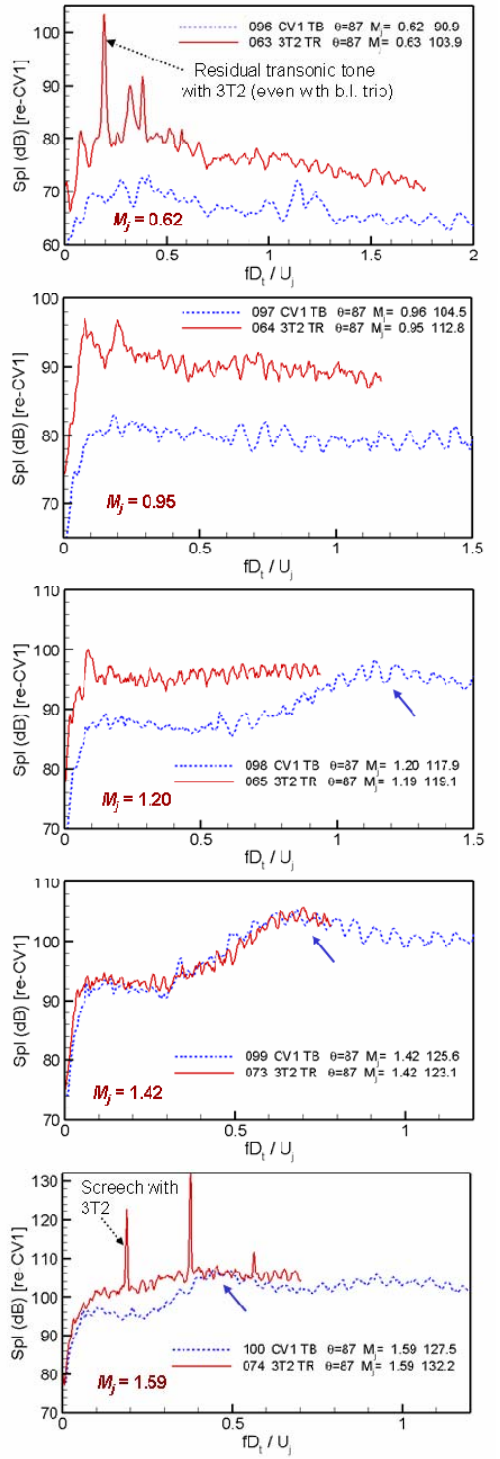

Fig. 9 SPL spectra for nozzle 3T2 (M_D = 1.78) vs. convergent (CV1) case, at indicated M_j; θ = 90°.

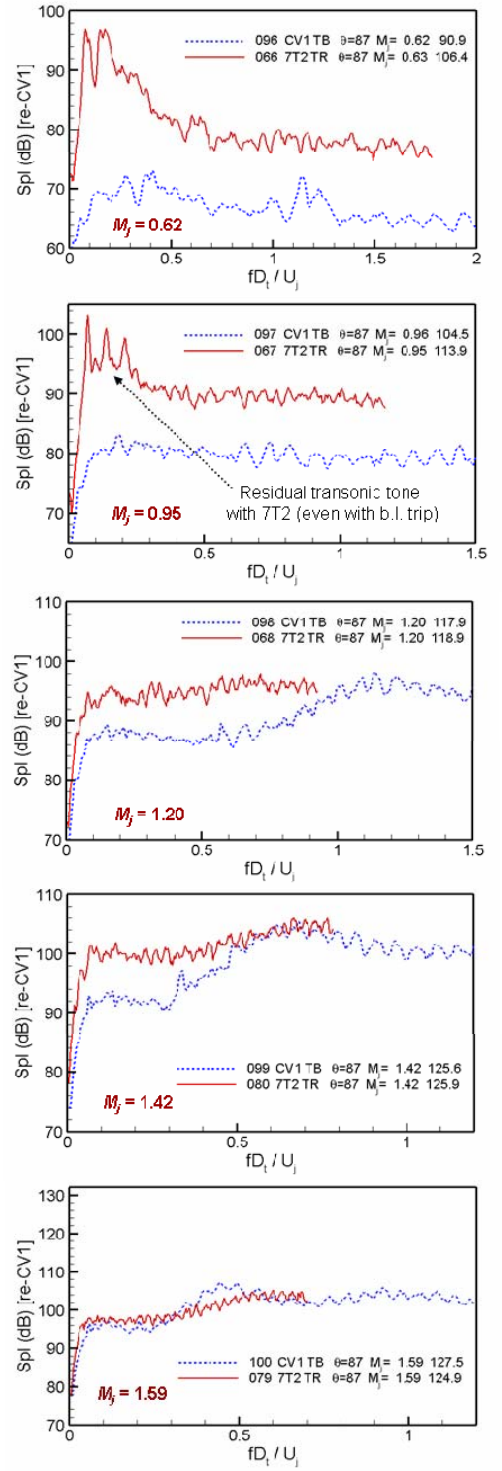

Fig. 10 SPL spectra for nozzle 7T2 (M_D = 2.78) vs. convergent (CV1) case, at indicated M_j; θ = 90°.

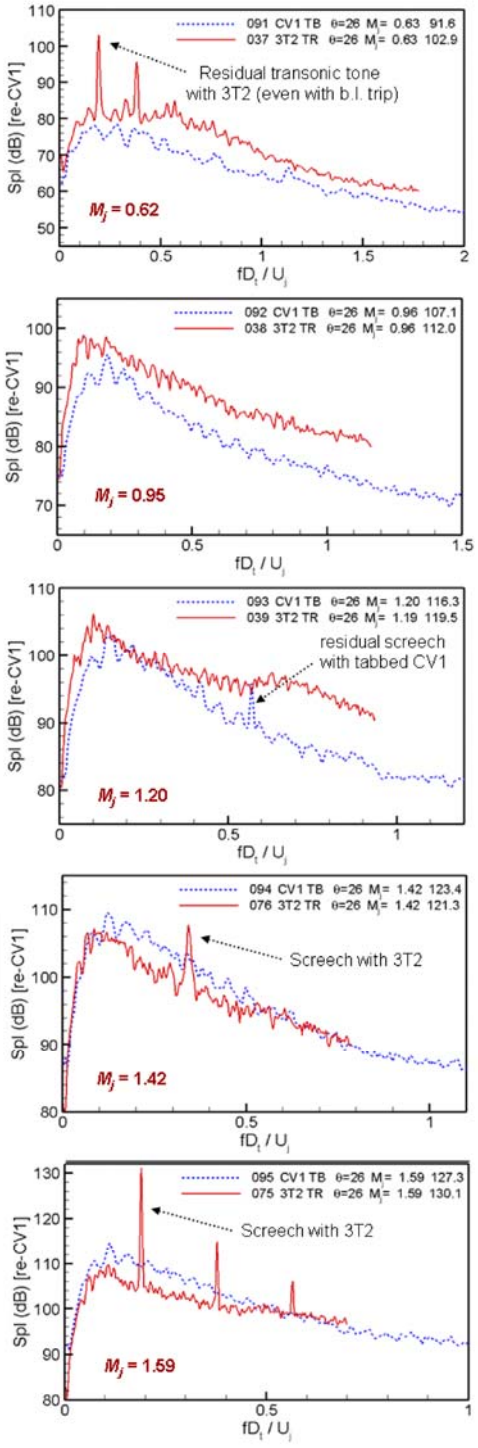

Fig. 11 SPL spectra for nozzle 3T2 (M_D = 1.78) vs. convergent (CV1) case, at indicated M_j; θ = 25°.

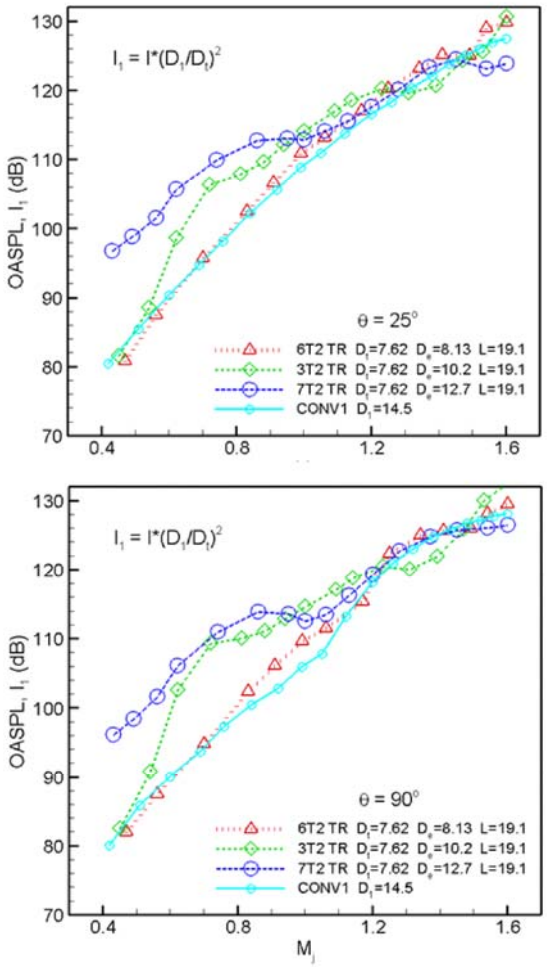

Fig. 12 OASPL vs. M_j for nozzles 3T2, 6T2 and 7T2 compared to convergent (CV1) case, at indicated polar locations (θ); data scaled to diameter of CV1.

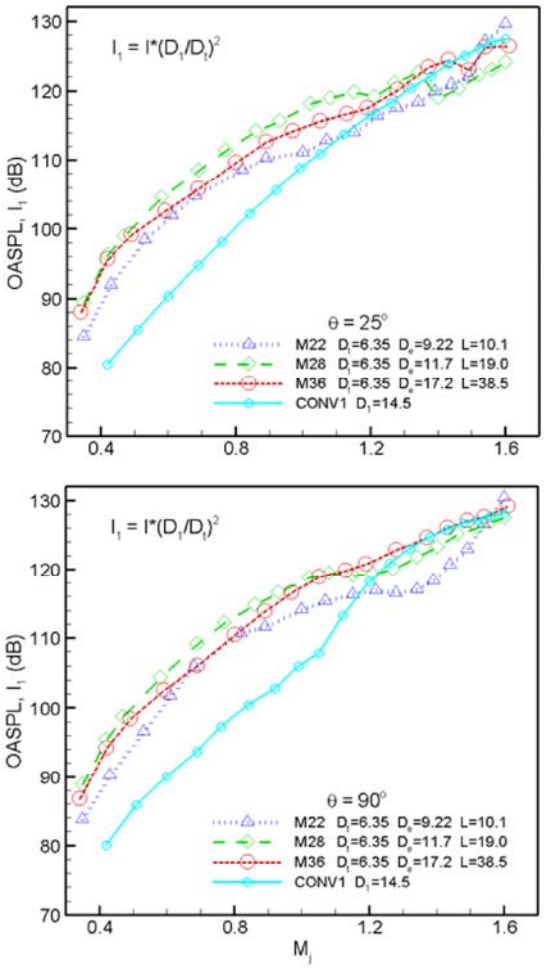

Fig. 13 OASPL vs. M_j for 16° conical divergent section cases (M22, M28, M36) compared to convergent (CV1) case, at indicated polar locations (θ); data scaled to diameter of CV1.